Wiley
International Journal of Energy Research
Volume 2024, Article ID 8832086, 15 pages
https://doi.org/10.1155/2024/8832086

WILEY

Research Article

The Effect of Converting a Conventional Tractor into a Hybrid Drive Tractor Using the ECMS Method on Fuel Consumption and Emissions

Mirac Ozturk,[1] **Tarkan Sandalci**,[1] **Cihan Buyuk**,[2] **Mustafa Guclu**,[2] and **Yasin Karagoz**[3]

[1]*Department of Mechanical Engineering, Yildiz Technical University, Besiktas, Istanbul, Türkiye*
[2]*Tumosan Company, Istanbul, Türkiye*
[3]*Department of Mechanical Engineering, Istanbul Medeniyet University, Istanbul, Türkiye*

Correspondence should be addressed to Yasin Karagoz; yasin.karagoz@medeniyet.edu.tr

Received 29 May 2024; Accepted 23 August 2024

Academic Editor: Paolo Castaldo

In recent years, the implementation of Tier 5 emission regulations for tractors has compelled manufacturers to conduct new research. Additionally, the process of hybridization has impacted the agricultural vehicle industry. This study focuses on the design and implementation of an energy management strategy (EMS) for a diesel–electric hybrid electric agricultural vehicle, based on real-time optimization. Tractor drive systems, including both conventional and hybrid options, were introduced. Simulations were performed to compare fuel consumption and CO_2 emissions between the two types of tractors. The data shows that hybrid vehicles produce 8.93% less CO_2 than conventional vehicles. Furthermore, the fuel consumption of the tractor decreased from 1,880.2 to 1,712.5 g/km under hybrid operating conditions.

1. Introduction

The modern agricultural industry has evolved to prioritize electricity, environmental sustainability, and innovation in line with advancements in the quality of life [1, 2]. Hybrid tractors, which combine a combustion engine and an electric motor, are designed to decrease fuel consumption and emissions while maximizing fuel efficiency [3, 4]. These tractors have become a primary area of research in the agricultural industry due to their ability to optimize fuel efficiency and reduce emissions. This benefits the environment and helps farmers and agricultural businesses save on operating costs. Additionally, hybrid tractors that promote sustainable agricultural practices play an important role in preserving natural resources [5].

Compared to internal combustion engines alone, the hybrid power system in robotic tractors for precision agriculture reduces exhaust emissions by almost 50% [3]. Mocera and Martini [6] proposed a hybrid tractor architecture and investigated the performance numerically. The hybrid electric continuously variable transmission (HeCVT) agricultural tractor demonstrates strong peak power and consistent fuel efficiency when compared to conventional diesel tractors in typical daily work scenarios. To achieve better performance, many researchers have studied on energy management strategies specifically for dual-motor drive systems in tractors. Energy management strategies (EMS) in hybrid tractors aim to optimize the use of the internal combustion engine (ICE) and electric motor (EM) to maximize fuel efficiency.

EMS can be divided into three categories, namely rule-based, optimization-based, and learning-based [7]. Rule-based strategies use predefined rules or logic to make decisions [8, 9]. The current energy management strategies are dominated by rule-based approaches due to their simplicity, reliability, ease of implementation, and interpretability [10, 11, 12]. Optimization-based strategies are divided into two algorithms: global optimization and real-time optimization [13]. These strategies provide increased adaptability, flexibility, and efficiency, especially in complex and dynamic environments. Real-time optimization aims to minimize energy consumption

Table 1: A brief review of the literature.

Reference	Vehicle and study	Research focus	Solution approach
Mocera and Martini [6]	Numerical study using downsized engine	Using eCVT in hybrid tractor	Numerical control methods using different control strategies
Zhu et al. [15]	Numerical study with ECMS	Hydro-mechanical continuously variable transmission (HMCVT)	A fuzzy adaptive equivalent fuel consumption minimization strategy (FA-ECMS)
Zhu [16]	Experimental and numerical study	Design a parallel hydraulic hybrid system for a heavy terminal tractor	Dynamic rule-based control strategy
Xie et al. [17]	Numerical study for ANN supported ECMS	Developing ANN for ECMS	Developing ANN to regulate the equivalent factor improving the management effectiveness of the equivalent consumption minimum strategy (ECMS)
Jia et al. [18]	Numerical study	Developing numerical methods for optimal control of hybrid electric agricultural tractors	Optimization-based energy management strategies for HEATs to minimize the fuel consumption
This study	Experimental and numerical study	Downsizing the engine using a 3-cylinder ICE in P2 hybrid operating mode and developing a control strategy for parallel hybrid configuration	Equivalent fuel consumption with both P2 hybrid conversion and ECMS

during energy management by using the engine's optimal working curve, which includes fuel consumption, power, and efficiency, to find the best working point for controlling the variables of hybrid/electric vehicles. This ensures that both the engine and electric motor operate at their optimal state. The real-time optimization strategy does not require knowledge of future driving information and is not limited by specific driving cycle conditions [14].

Zhu et al. designed a parallel-hybrid tractor system that employs a hydro-mechanical continuously variable transmission (HMCVT). The system's power distribution is achieved through the use of a fuzzy adaptive equivalent fuel consumption minimization strategy (FA-ECMS) [15]. This strategy dynamically adjusts the equivalence factor in real-time, allowing for a more reasonable power distribution. Zhu [16] presented a design for a parallel hydraulic hybrid heavy terminal tractor. The authors proposed a dynamic rule-based control strategy that improves fuel economy by 38.1%–61.6% compared to conventional designs. Xie et al. [17] developed an ANN to regulate the equivalent factor improving the management effectiveness of the ECMS. Jia et al. [18] discussed the use of numerical methods for optimal control of hybrid electric agricultural tractors. The focus was on reducing fuel consumption during typical working cycles through optimization-based energy management strategies. Overall, the literature indicates that hybrid technology has the potential to significantly improve tractor fuel economy, with both economic and environmental advantages. On the other hand, there are different application areas and studies in the literature regarding energy management strategies related to hybrid vehicles. Han et al. [19] in their study, they examined the effect of battery charging and discharging efficiencies in electric hybrid vehicles in cold weather. As a result of their research, they concluded that the efficiency increased significantly with the battery heating system in cold weather. Han et al. [20] in another study, they developed a speed prediction model for hybrid electric vehicles by taking battery aging into account with a predictive control-based model.

In order to achieve sustainable agriculture, it is essential to minimize energy consumption and the harmful effects on the environment. Energy efficiency and fuel economy in tractors are of great importance for farmers and sustainable agriculture. In this context, although there are many publications about vehicles in the literature, studies on hybrid operation in tractors are quite limited. For this reason, the strategy was studied based on equivalent fuel consumption with both P2 hybrid conversion and ECMS. In addition, a more realistic and commercially usable system was studied by studying P2 class hybrid conversion and ECMS on the tractor. Also, a brief review of the literature can be seen in Table 1. In this study, the tractor performance regarding fuel economy and emissions for different operation cycles were compared by simulations. The study investigated the improvement in fuel consumption and CO_2 emissions by downsizing the engine using a 3-cylinder ICE in P2 hybrid operating mode and developing a control strategy for parallel hybrid configuration. Hybrid working areas and internal combustion engine working points were relocated to more suitable areas. The aim of the study is to develop an ECMS, based on vehicle speed and demanded torque value depended on field properties. The designed ECMS was evaluated using actual driving speed profiles on hard and soft soil conditions.

2. Materials and Method

This study consists of two parts: an experimental studies and modelling studies. The following section provides a detailed explanation of the experimental study and the GT-SUITE model for both hybrid and conventional vehicles.

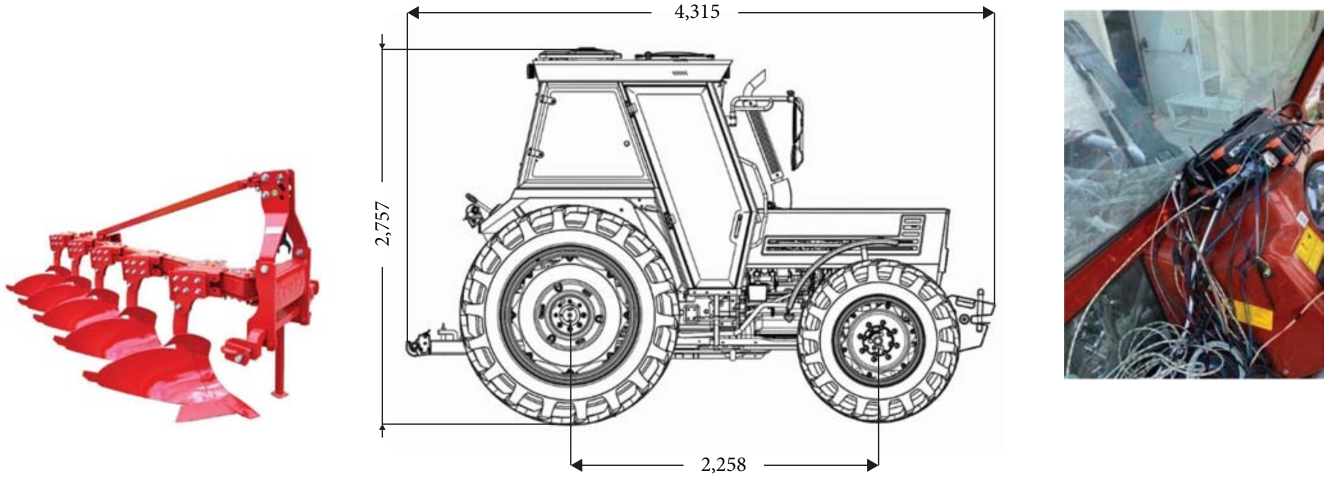

Figure 1: Moldboard plough, tractor, and data acquisition system.

2.1. Experimental Study

2.1.1. Field Tests. The study focused on ploughing, which is considered a low-speed, high-torque operation. Field tests were conducted on farms to collect primary research data. The tests were conducted in Konya (Figure 1), Turkey at an ambient temperature ranging between 25°C–30°C. Also, the altitude of the field is 1,016 m.

Tests were conducted in two different fields with soils of varying characteristics. One field, referred to as hard soil, required the engine map to operate in regions close to the full load curve by drawing more power. The other field, referred to as soft soil, required partial load and the engine to operate at partial loads.

The study employed a tractor weighing 3,500 kg with a 12F–12R transmission, with further details provided in Table 1. A 760 kg moldboard plough was used during the tests (Table 2 for plough details).

Tests were conducted in two different fields with soils of varying characteristics, as shown in Figure 2. One field, referred to as hard soil, required the engine map to operate in regions close to the full load curve by drawing more power. The other field, referred to as soft soil, required partial load and the engine to operate at partial loads.

The data acquisition system was installed on the tractor and connected directly to the diesel engine control unit. The CAN information received from the ECU and the pressure, flow, and rpm values obtained from the engine were collected by the DEWESOFT SIRIUS HS and SIRIUS HS LV + device. The KRYPTONi 16xTH device was used to collect temperature and fan speed information from the engine.

Torque, power, fuel consumption, engine oil temperature and pressure values, mass air flow, turbo outlet temperature and pressure values, exhaust gas temperature and exhaust emission values were measured and recorded, and engine maps were created based on different load (% pedal) and engine speeds.

Two different engines were used in the field tests: a 95 HP engine in the conventional vehicle and a 75 HP engine in the hybrid vehicle.

Table 2: Tractor vehicle and moldboard plough specifications.

Tractor	Total weight (kg)	3,500
	Frontal area (m^2)	3.5
	Transmission	12F + 12R
	Weight distribution (%)	Front 40 Rear 60
	Front tire	380/70R24
	Rear tire	420/85R34
Moldboard plough	Total weight (kg)	760
	Working width (m)	1.5
	Moldboard width (cm)	35
	Number of moldboard	5

A driving cycle was created using real data collected from the tractor during ploughing operations in both soft and hard soil conditions. Details for data in the driving cycle are provided in Figure 2. Due to the low speed and high-power demand, the engine operates at high torque region.

The speed of the tractor varies between 5 and 8 km/hr during the ploughing operation.

2.1.2. Engine Dynamometer Tests. A dynamometer was used to measure to torque and rotational speed of the engines. The engine speed–torque curves were generated by analyzing data collected from a dynamometer. The measurements were taken at different motor speeds to demonstrate the correlation between motor speed and torque output. This aids in understanding and optimizing engine performance.

During the internal combustion engine tests, the engine was connected to an active dynamometer (AVL Dyno Road 402) via a shaft. The engine cooling water was conditioned at 80°C using AVL Consyscool. AVL ConsysBoost device was used to fix the engine intake air temperature at 55°C, while the fuel temperature was maintained at 40°C (AVL 753C) during the tests. Test were carried out for 4-cylinder 95 HP and 3-cylinder 75 HP engines as given in Figure 3.

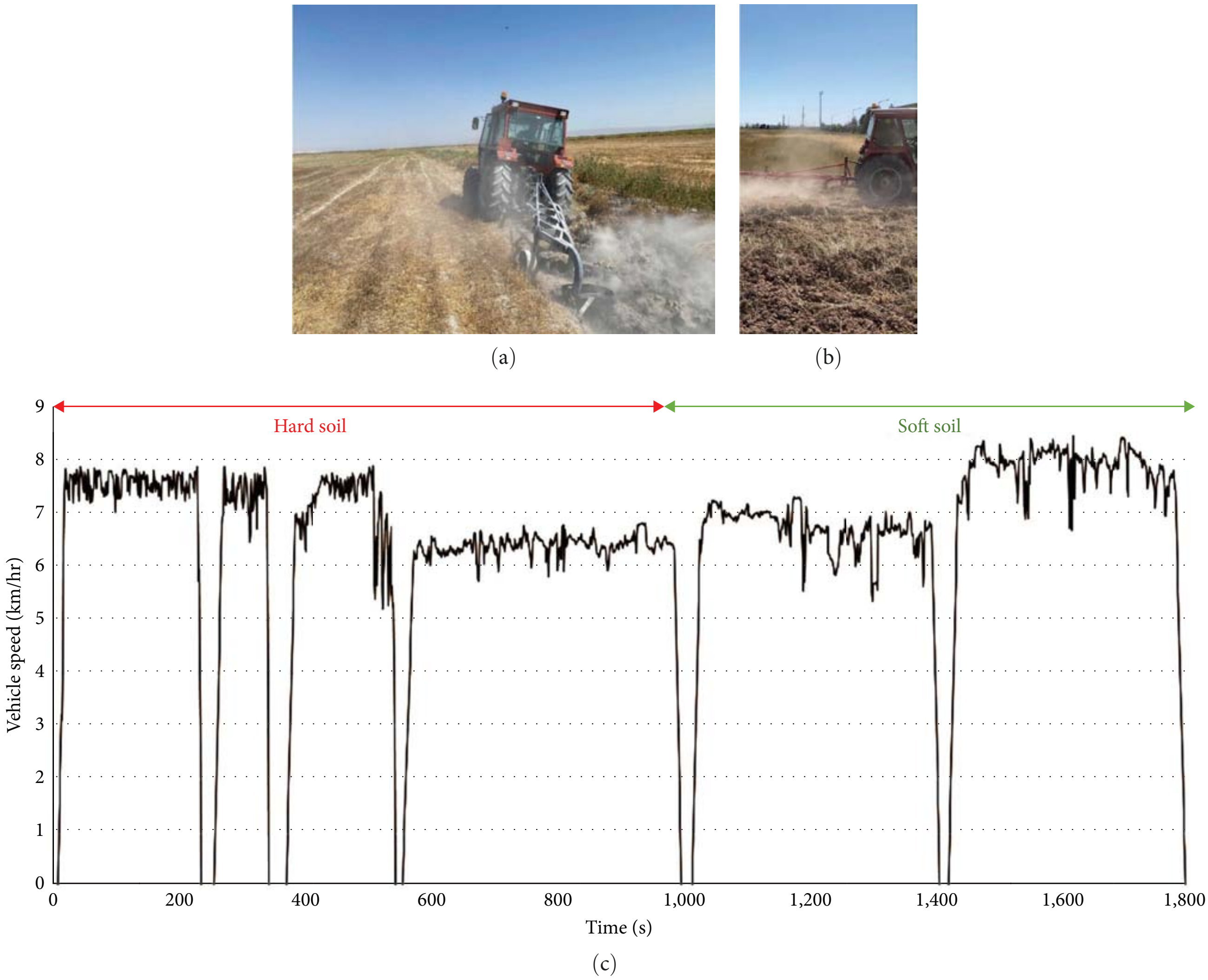

Figure 2: Ploughing operations on (a) hard soil, (b) soft soil, and (c) driving cycle of the tractor.

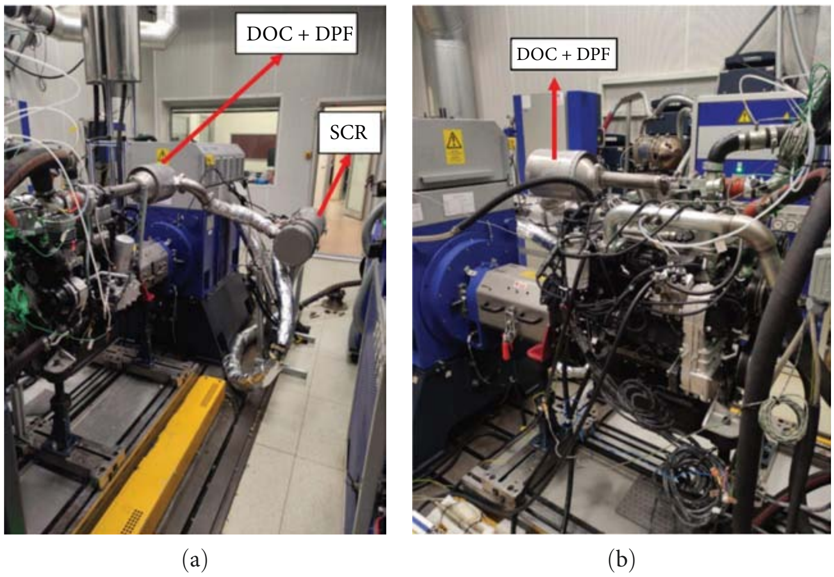

Figure 3: Dynamometer tests for (a) 4-cylinder 95 HP and (b) 3-cylinder 75 HP engine.

TABLE 3: 4-cylinder 95 HP diesel engine specifications.

Total displacement (cc)	3,900
Rated power (kW) @ 2,200 rpm	70
Rated torque (Nm) @ 1,400–1,650 Rpm	400
Rated speed (rpm)	2,550

2.1.3. 4-Cylinder 95 HPEngine Performance and Fuel Consumption Maps. The rated power and torque of the diesel engine are 70 kW and 400 Nm, respectively. The features are listed in the Table 3.

Table 3 shows that the engine used is a diesel internal combustion engine specifically designed for the tractor, with high torque. It provides the rated torque at a low speed of 1,400–1,600 rpm and can deliver a power of 70 kW (95 HP) with its 4 cylinders.

Torque and BSFC maps of the engine were created at different speeds and pedal positions. Figure 4 displays the break engine torque in relation to the pedal position and engine speed. This allows for the estimation of torque values during field tests based on the pedal position and engine speed.

Figure 4 also presents BSFC values at various engine speeds and torques. The engine map is three-dimensional, and it shows that specific fuel consumption decreases to 225 g/kWh in the engine's most efficient operating region, also known as the egg curve in the literature. In the least efficient operating region, it can reach up to 450 g/kWh.

2.1.4. 3-Cylinder 75 HP Engine Performance and Fuel Consumption Maps. The rated power and torque of the diesel engine are 55 kW and 300 Nm, respectively. The features are listed in Table 4. Torque and BSFC maps of the engine were created at different speeds and pedal positions.

Figure 5 shows the engine torque at different pedal positions and engine speeds, allowing for the extraction of specific fuel consumptions when connected to the dynamometer. The engine exhibits lower power and torque performance due to its three cylinders.

Figure 6 presents BSFC values at various engine speeds and torques. The specific fuel consumption decreases up to 215 g/kWh in the most efficient operating region of the three-dimensional engine performance map, while it reaches up to 450 g/kWh in the most inefficient working area.

It is observed that the 3-cylinder engine achieves lower specific fuel consumption at the same power compared to the 4-cylinder engine.

2.1.5. Hybrid Tractor Configuration and Electric Motor and Battery Selection. Figure 7 presents a schematic of a P2 class hybrid tractor propulsion system. The system comprises a 20 kW electric motor with a driver, a Li-ion battery rated at 120 Ah and 250 V. As this is a P2 class hybrid configuration, the electric motor is located between the clutch and the transmission.

The hybrid system is designed to operate with the electric motor at low loads and speeds, use both the electric motor and the internal combustion engine across the full load curve, and charge the battery efficiently based on its state of charge (SOC) status.

2.1.6. Electric Motor and Battery Specification. Table 5 presents the specifications for the electric motor and battery pack. The chosen electric motor is an asynchronous motor with a power of 20 kW, a rated speed of 3,000 rpm, and a torque of 170 Nm. The battery pack has an energy capacity of 120 Ah, a rated voltage of 250 V, and a total capacity of 30 kWh.

Figure 8 displays the maximum torque curves for the 3-cylinder 75 HP diesel engine, the 4-cylinder 95 HP diesel engine, and the hybrid system (3-cylinder 75 HP diesel + electric motor). It is evident from the figure that in the hybrid operating condition, the maximum torque curve at full load exceeds that of the 4-cylinder engine.

2.2. Modelling Study (GT-SUITE Model). The effectiveness of the proposed ECMS is verified using the GT-SUITE test platform. GT-SUITE model includes many submodels including vehicle dynamics, engine type, and driver behavior. The model's validity was assessed by evaluating its output variables and comparing it with experimental data.

2.2.1. Conventional Vehicle Model. Figure 9 schematizes the conventional tractor topology. The vehicle model comprises fundamental components: the driver, the environment model, the engine, and the vehicle powertrain.

The figure illustrates that in the conventional tractor vehicle model, separate submodels are used for the transmission, engine, driver, and vehicle. This approach enables the collection of fuel consumption and emission data based on travel resistance.

Figure 10 shows that the maximum power of the diesel engine during ploughing work is 61.46 kW. The figure illustrates that the instantaneous power requirement varies dynamically depending on the driving cycle during field tests. The power requirement was determined based on time as a result of tests conducted in two different soil fields, hard and soft.

2.2.2. Conventional Engine Maps and Operating Points. Operating points and full load curve of 95 HP diesel engine is given in Figure 11. Engine has large working area. The figure shows that the engine operates intensively at partial loads and in regions with lower efficiency and high specific fuel consumption. It is expected that a conventional vehicle's total fuel consumption may increase because the engine operates in regions with high fuel consumption.

2.2.3. Hybrid Vehicle Model. A hybrid tractor is an integrated system that consists of mechanical, electrical, and hydraulic components. It has two driving systems; a diesel engine and an electric motor. Programmed electronic control units optimize the vehicle's performance and efficiency by managing the switching between different operating configurations. In comparison to conventional tractors, optimal control of power distribution technique in parallel hybrid tractors can significantly increase fuel efficiency and traction performance [21].

Figure 12 shows the powertrain of the hybrid tractor consisting diesel engine, electric motor, and battery pack.

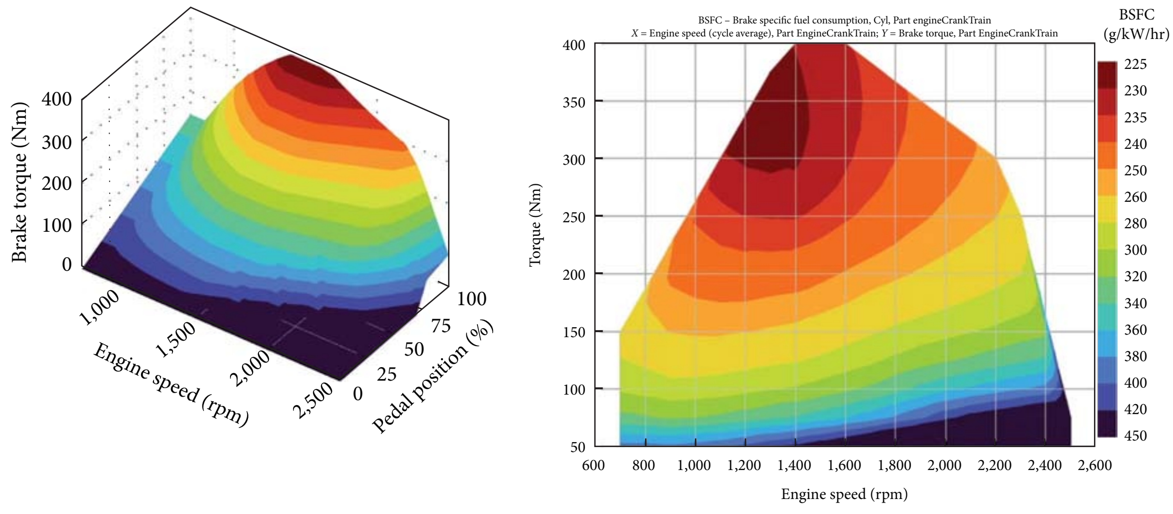

(a) (b)

Figure 4: 4-cylinder 95 HP engine (a) torque values depend on engine speed and pedal position and (b) BSFC map depend on engine speed and brake torque.

Table 4: 3-cylinder 75 HP diesel engine specifications.

Total displacement (cc)	2,900
Rated power (kW) @ 2,200 rpm	55
Rated torque (Nm) @ 1,400–1,750 Rpm	300
Rated speed (rpm)	2,550

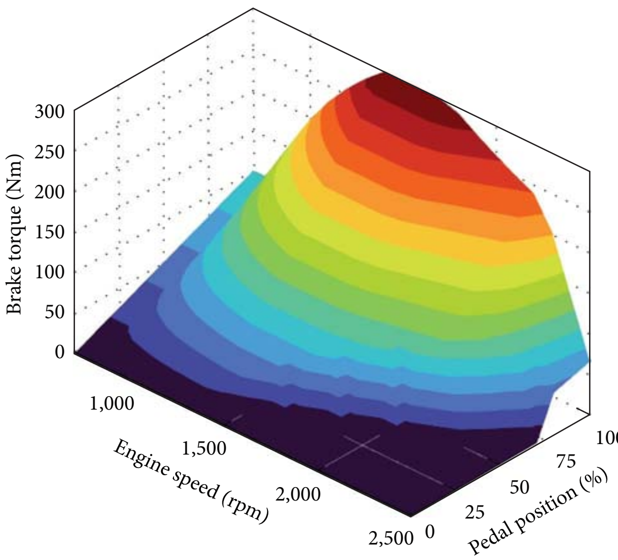

Figure 5: 3-cylinder 75 HP engine torque values depend on engine speed and pedal position.

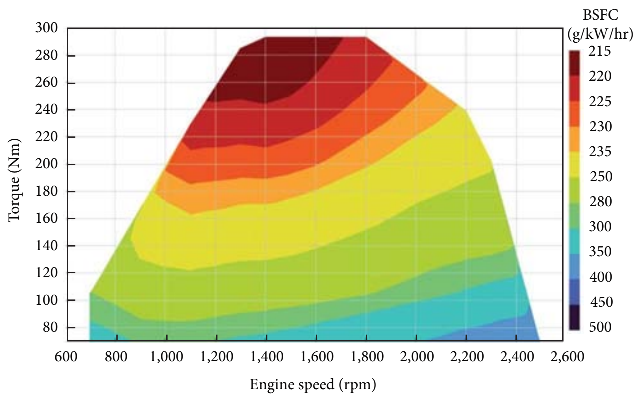

Figure 6: 3-cylinder 75 HP BSFC map depend on engine speed and brake torque.

Weight gain was achieved in the hybrid model as a result of the removal of the SCR system used in the conventional model. The hybrid model uses a battery and electric motor instead of a tank and catalyst in the conventional model, resulting in a negligible change in the weight of both tractors. Therefore, the same weight was used for both models. Thevenin electrical-equivalent battery model was used in this model. An electric motor weighing 45 kg with a rated power of 20 kW and a Li-ion battery weighing 280 kg with a power of 30 kWh were used. On the other hand, there is an additional load of 330 kg in total with the driver and other equipment. On the other hand, instead of the 4-cylinder 95 HP engine, a 3-cylinder 75 HP engine was used. While a 4-cylinder 95 HP diesel engine weighs 420 kg, a 3-cylinder 75 HP diesel engine weighs 340 kg. In this case, by converting the tractor to a hybrid, the vehicle weight increases by 250 kg.

2.2.4. Hybrid Engine Map and Operating Points. The hybrid vehicle does not utilize the SCR system, but it still meets the stage five emission standard through engine calibration. The volume that would have been occupied by the SCR system was instead used for the battery and EM.

To improve efficiency, a 3-cylinder engine was selected for the hybrid system, resulting in reduced engine power and the ability to operate at more efficient points on the map.

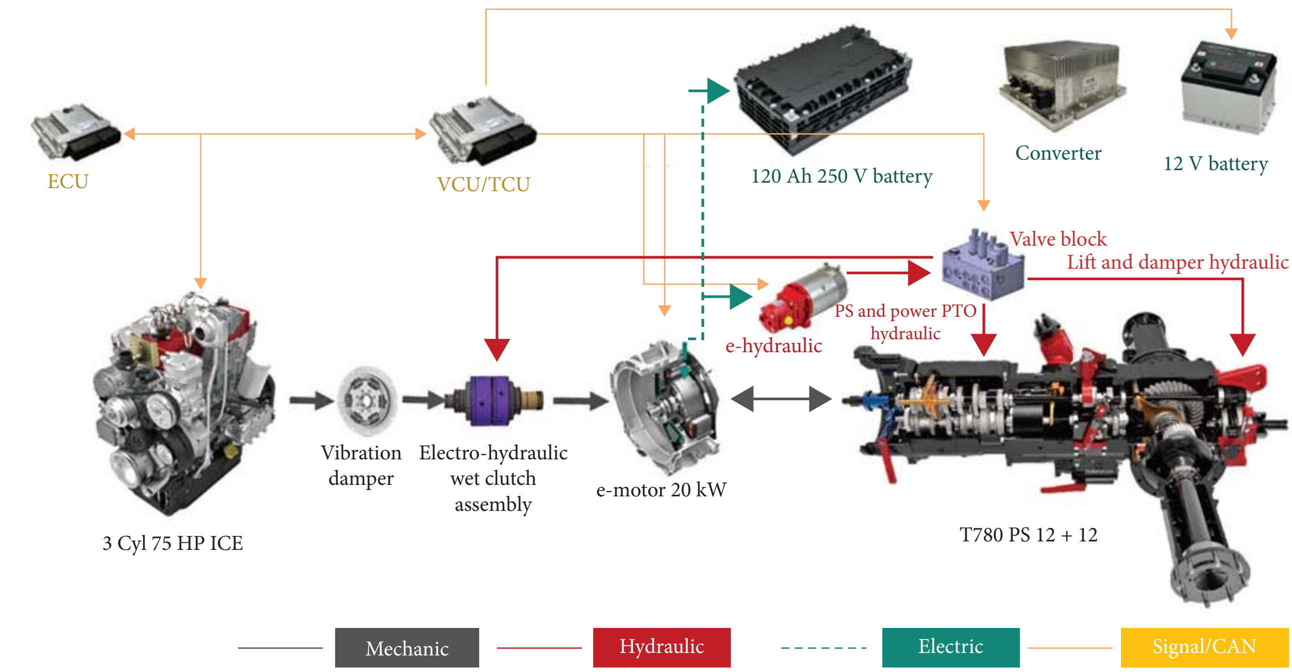

Figure 7: P2 mild hybrid concept.

Table 5: Electric motor and battery pack specifications.

Electric motor	Rated power (kW)	20
	Rated speed (rpm)	3,000
	Rated torque (Nm)	170
Battery pack	Energy capacity (Ah)	120
	Rated voltage (V)	250

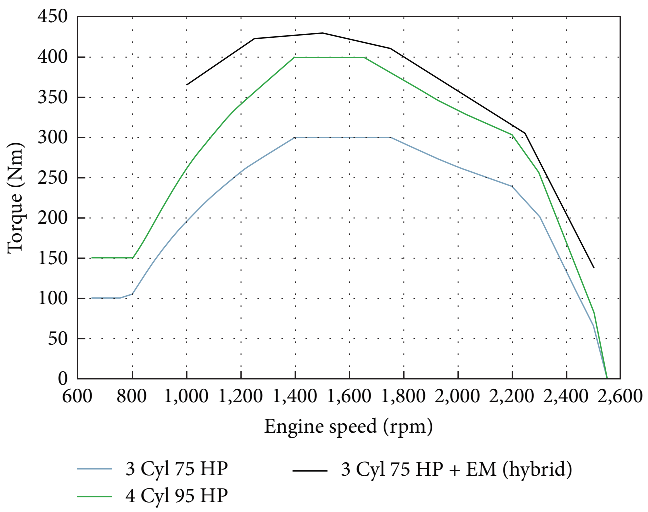

Figure 8: Full load curves for 3-cylinder 75 HP engine, 4-cylinder 95 HP engine, and hybrid configuration.

Figure 13 displays the full load curve and operating points for hybrid mode. The figure shows that in the hybrid operating condition, the internal combustion engine operates more intensively in regions with higher thermal efficiency and low specific fuel consumption, and is closer to the full load curve. This situation is expected to result in an improvement in total fuel consumption.

Figure 14 shows the SOC curve corresponding to plough operation. The x-axis of the figure is 1,800 s, which indicates a period of time for testing.

As can be seen from the figure, the SOC has returned to its initial value of 0.5.

It is clear that the battery is alternating between discharging and recharging. The Figure 15 illustrates the charging status of the electric motor and the SOC value of the battery under varying power demands. The negative curves of the electric motor indicate the charging state.

Maintaining an optimal SOC is crucial for both the range of the drive cycle and the battery's longevity. Considering the cost of electrical power helps ensure the SOC is maintained at optimum level [22].

Figure 16 shows the change of electric engine, internal combustion engine, and auxiliary power demand depending on the SOC value depending on the cruise cycle.

2.3. Data Reduction. Using the basic equations of motion and conservation of energy, engine torque and power were calculated from the force transmitted to the vehicle drive wheels depending on the travel resistances. Details are given below.

Engine equation of motion (balances engine brake torque with engine inertia torque and engine side load torque from the clutch) is given in Equation (1).

$$T_{\mathrm{eng}} = \left[I_{\mathrm{eng}}\right] \frac{d\omega_{\mathrm{eng}}}{dt}. \quad (1)$$

Driveline equation (for speed of vehicle side of clutch, denoted as drv) is given in Equation (2). Balances vehicle side

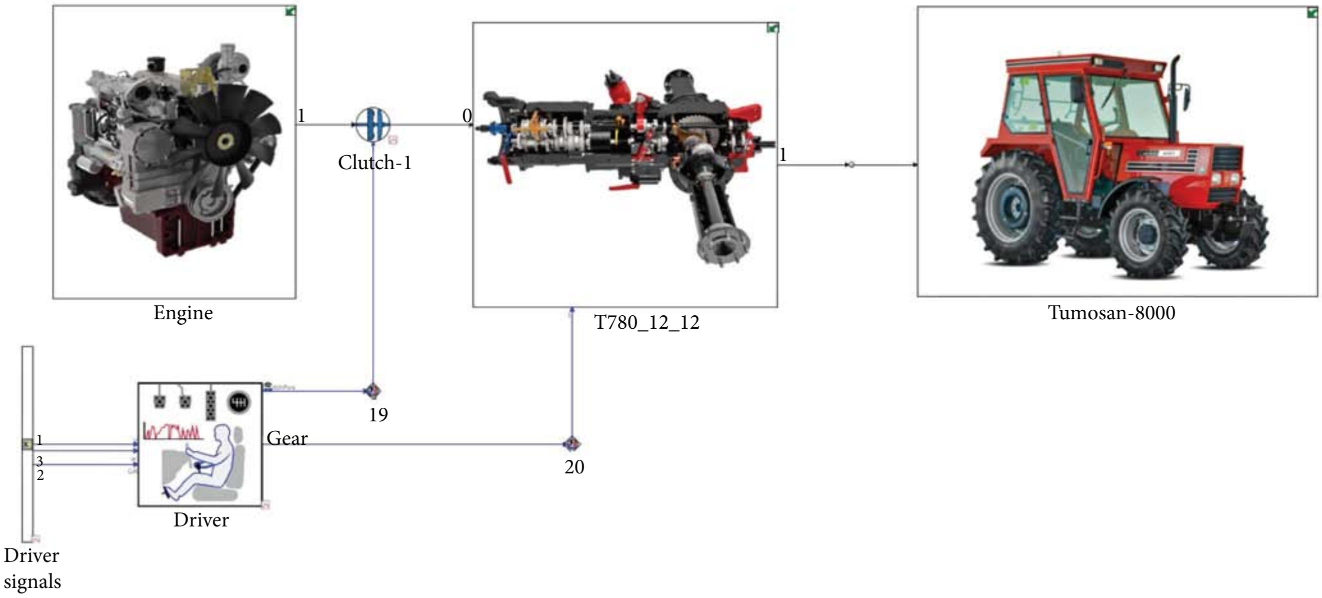

Figure 9: Conventional model.

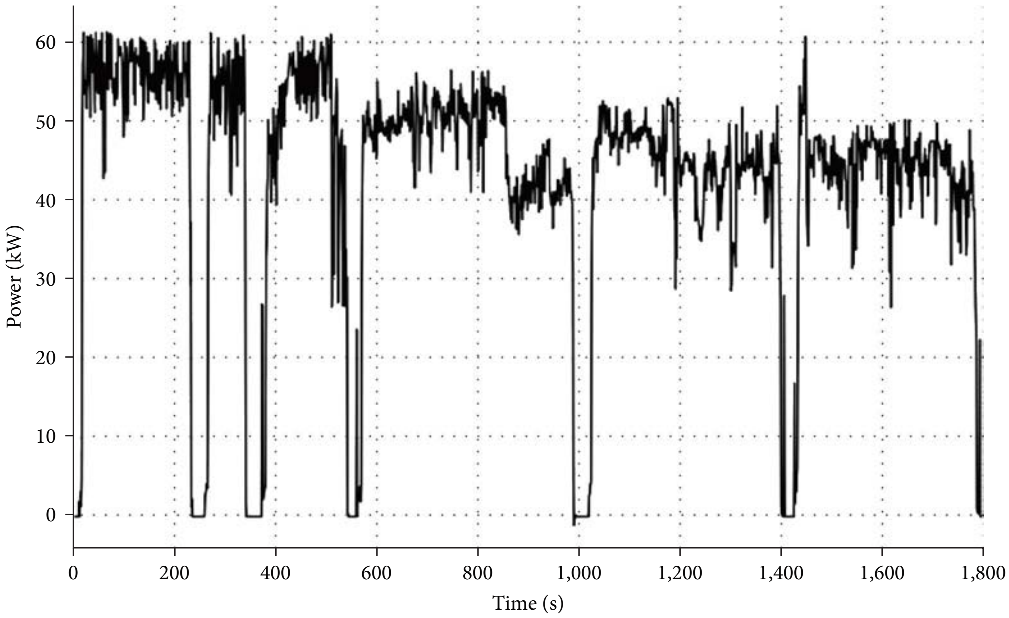

Figure 10: Conventional engine power–time curve.

output torque from clutch with inertia torque of the entire driveline and vehicle and the effective torque of the retarding (aerodynamic, rolling resistance, and grade) forces on the vehicle:

$$T_{\mathrm{drv},v} = \left[I_{\mathrm{trans1}} + \frac{I_{\mathrm{trans2}}}{R_t^2} + \frac{I_{\mathrm{dsh}}}{R_t^2} + \frac{I_{axl}}{R_d^2 R_t^2} + \frac{M_{\mathrm{veh}} r_{\mathrm{whl}}^2}{R_d^2 R_t^2}\right] \frac{d\omega_{\mathrm{drv}}}{dt} - \left[\frac{I_{\mathrm{trans2}}}{R_t^3} + \frac{I_{\mathrm{dsh}}}{R_t^3} + \frac{I_{\mathrm{axl}}}{R_d^2 R_t^3} + \frac{M_{\mathrm{veh}} r_{\mathrm{whl}}^2}{R_d^2 R_t^3}\right] \omega_{\mathrm{drv}} \frac{dR_t}{dt} + \left[\frac{F_{\mathrm{aer}} + F_{\mathrm{rol}} + F_{\mathrm{grd}}}{R_d R_t}\right] r_{\mathrm{whl}}. \tag{2}$$

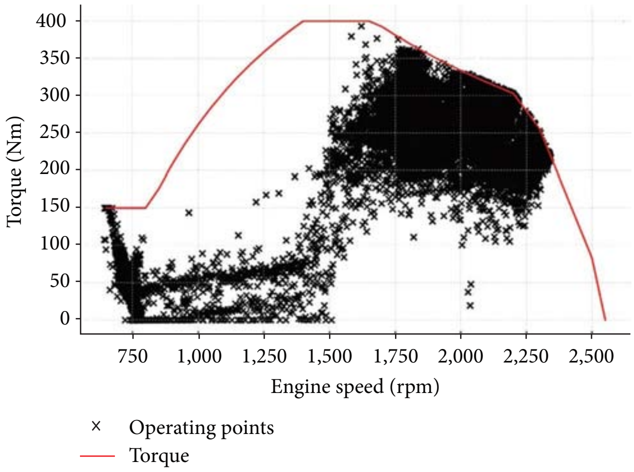

Figure 11: Operating points.

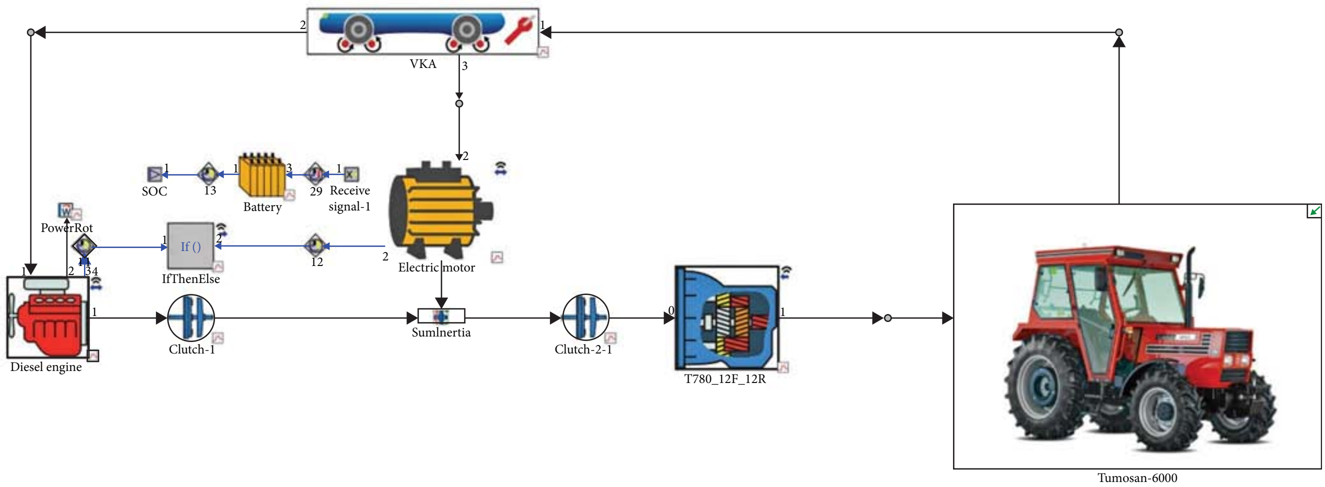

Figure 12: Hybrid model.

Additionally, aerodynamic resistance, rolling resistance, and hill resistance force calculations are given in Equations (3), (4), and (5), respectively.

$$F_{aer} = \frac{1}{2} \times \rho \times V^2 \times A_{frontal}. \quad (3)$$

$$F_{rol} = d_{road} \times c_{roll}(M_{veh} + M_{load}) \times g \times \cos \alpha. \quad (4)$$

$$F_{grd} = (M_{veh} + M_{load}) \times g \times \sin \alpha. \quad (5)$$

In the equations, ρ is the air density, d_{road} is the rolling resistance factor, c_{roll} is the rolling resistance factor, M_{load} is the vehicle mass, g is the gravitational acceleration, α is the road slope, V is the relative velocity of the air at the front of the vehicle, $A_{frontal}$ is the area of the front of the vehicle, T_{eng} is the engine braking torque, I_{eng} is the engine inertia torque, ω_{eng} engine speed, $T_{drv,v}$ clutch torque, I_{trans1} transmission inertia moment input, I_{trans2} transmission inertia moment output, I_{dsh} driveshaft inertia, I_{axl} axle moment, r_{whl} wheel radius, R_d transmission ratio, ω_{drv} driveline speed.

The following equations (Equations (6) and (7)) were used in the battery model. Instantaneous current through the open circuit voltage (I_{OC}) is integrated over time to calculate a change in capacity over the duration of the simulation. This change in capacity is subtracted from the initial capacity to calculate an instantaneous capacity.

$$\text{Cap}(t) = \text{Cap}_{\text{int}} - \int_0^t I_{OC} dt. \quad (6)$$

$$\text{Cap}_{\text{int}} = \text{SOC}_{\text{int}} \times \text{Cap}_{\text{max}}. \quad (7)$$

The battery's SOC is then defined as the ratio of instantaneous capacity to maximum capacity. It is calculated as in Equation (8) below.

$$\text{SOC} = \frac{\text{Cap}(t)}{\text{Cap}_{\text{max}}}. \quad (8)$$

In the equation, I_{OC} is the instantaneous current through the open circuit voltage value, Cap_{int} is the initial capacity

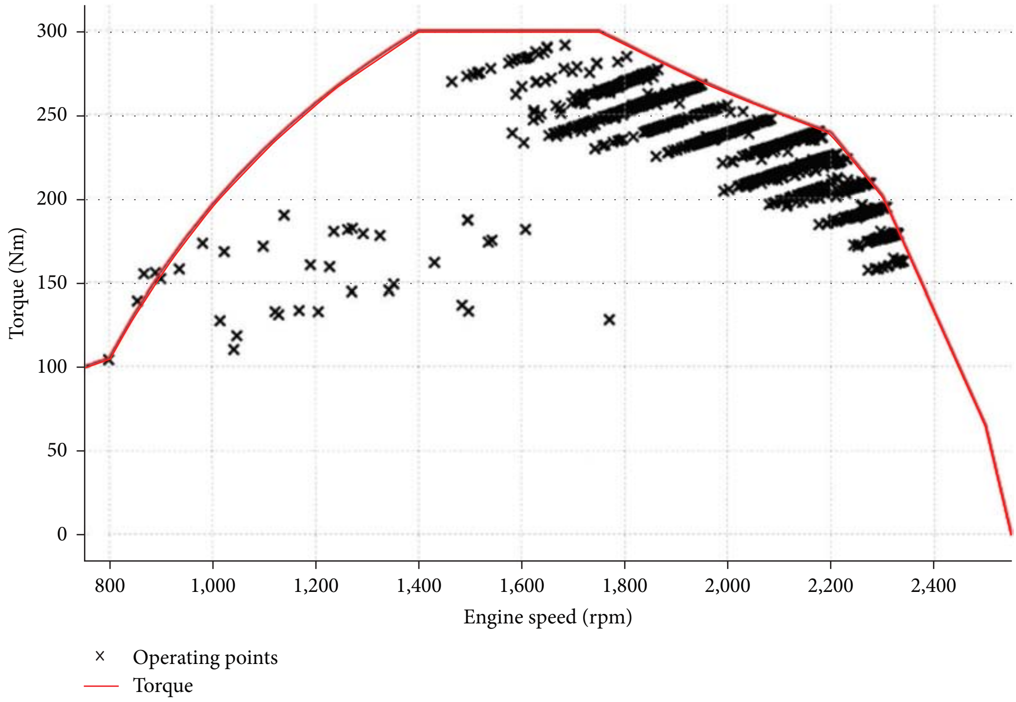

FIGURE 13: Hybrid vehicle engine operating points.

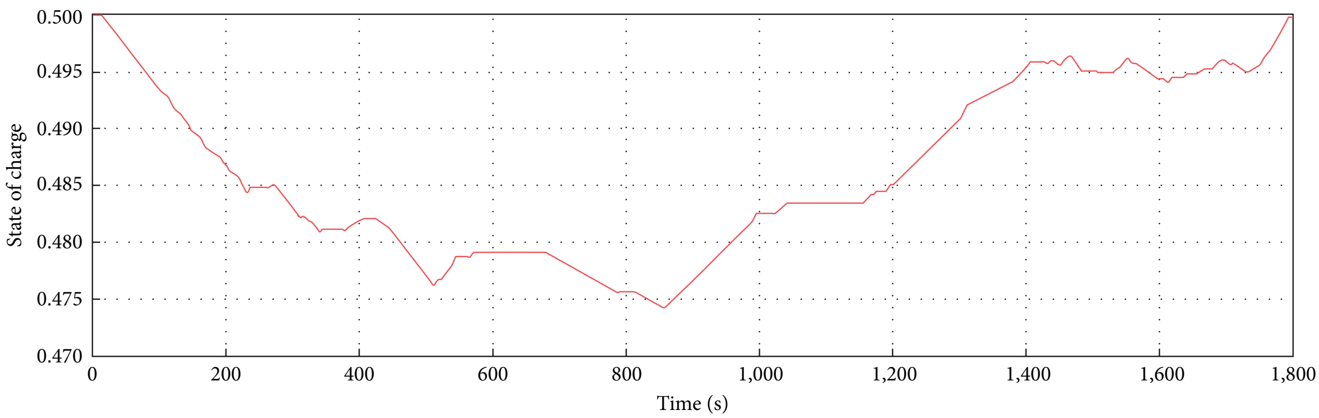

FIGURE 14: Change in state of charge over time.

value, $\mathrm{Cap}(t)$ is the instantaneous capacity value, $\mathrm{Cap}_{\max}$ is the maximum capacity value, $\mathrm{SOC}_{\mathrm{int}}$ is the initial state of charge value, and SOC is the state of charge gives its value.

2.4. ECMS. The primary benefit of an energy management strategy is the efficient distribution of fuel and electrical power to minimize fuel consumption [23, 24]. Hybrid tractors are a promising solution for achieving equivalent consumption minimization in the agricultural sector while maintaining the same level of performance.

An energy management strategy based on instantaneous optimization was designed and presented below.

According to the control algorithm strategy, the energy management system will determine which energy sources to activate.

Equivalent fuel consumption ($\dot{m}_{\mathrm{eqv}}(t)$) [25] in Equations (6) and (7);

$$\dot{m}_{\mathrm{eqv}}(t) = \dot{m}_f(t) + \dot{m}_{\mathrm{batt}}(t), \tag{9}$$

$$\dot{m}_{\mathrm{eqv}}(t) = \dot{m}_f(t) + \frac{s(t)}{Q_{\mathrm{lhv}}} \times P_{\mathrm{batt}}(t) \times p(\mathrm{SOC}). \tag{10}$$

The fuel consumption of the engine is represented by $\dot{m}_f(t)$, while $s(t)$ is the equivalent factor. $P_{\mathrm{batt}}(t)$ refers to the battery terminal power, Q_{lhv} stands for the fuel lower heating value, and $p(\mathrm{SOC})$ indicates the penalty function as calculated below in Equation (8).

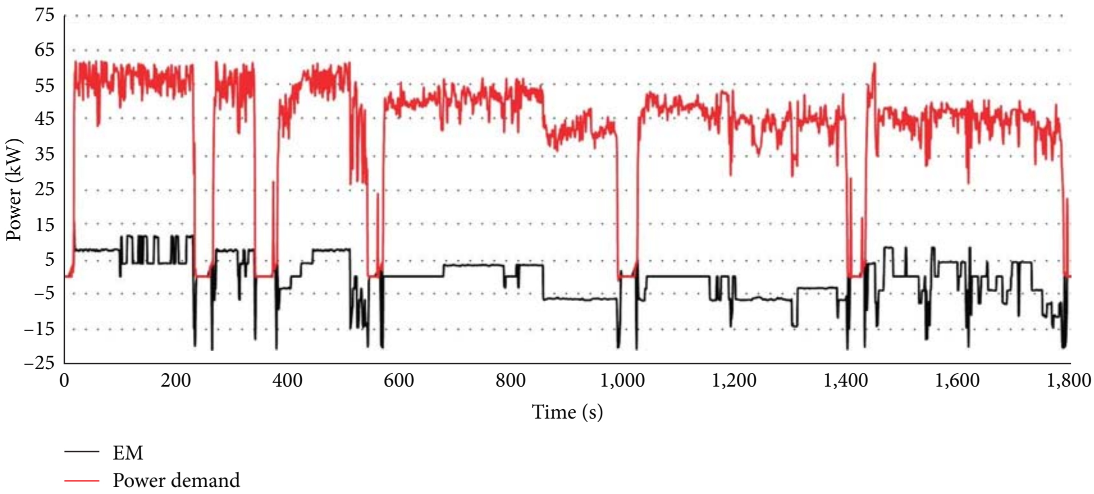

Figure 15: The charging status of the electric motor and the SOC value of the battery.

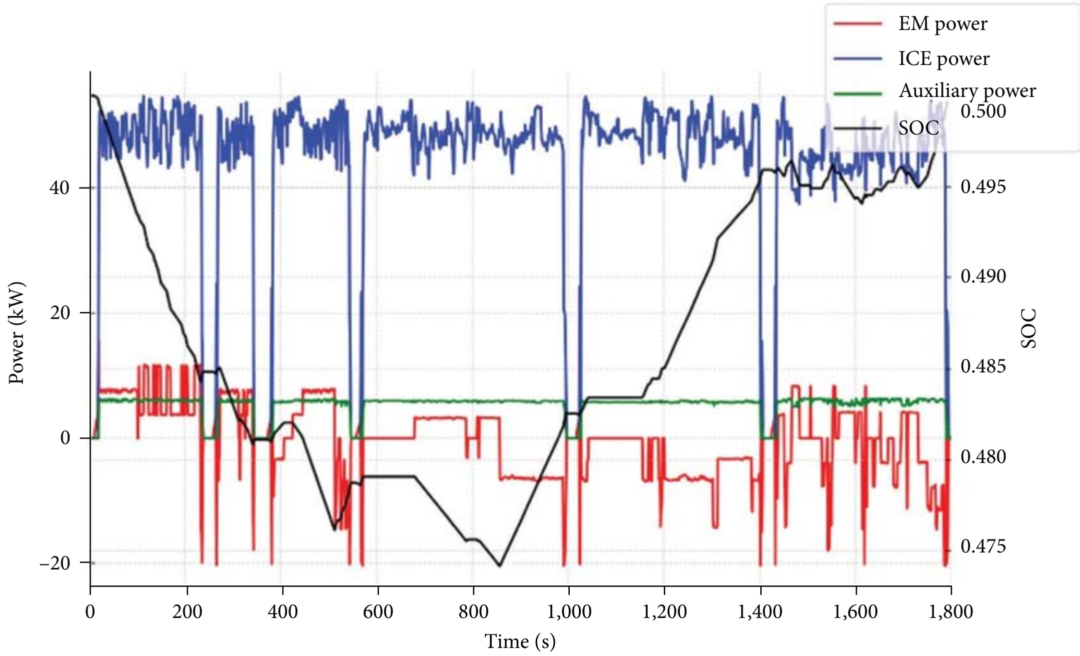

Figure 16: The comparison of electric motor power, ECE power, auxiliary power, and SOC.

$$p(\mathrm{SOC}) = 1 - \left(\frac{\mathrm{SOC}_{(t)} - \mathrm{SOC}_{(0)}}{(\mathrm{SOC}_{\max} - \mathrm{SOC}_{\min})/2}\right)^{\propto} \quad (11)$$

The model's charging state is designed to end at the same point where it started, allowing for a more accurate comparison in the cycle.

The tractor optimizes power and fuel economy by dynamically distributing the torque between the diesel engine and the EM based on the total power demand and the SOC value of the battery. This distribution is determined by the tractor's control strategy and algorithm.

Depending on the instantaneous power demand vehicle control system activates the hybrid mode, only ICE or pure electric modes, as appropriate. Operating regions are given in Figure 16 on the engine map.

Depending on the instantaneous power demand vehicle control system activates the hybrid mode, only ICE or pure electric modes, as appropriate. Operating regions are given in Figure 17 on the engine map.

The vehicle's control system activates hybrid, ICE-only or electric-only mode, depending on the instantaneous power demand and SOC value. If the SOC is above the minimum value, pure-electric mode is selected when the vehicle is started. Otherwise, if the battery is below the maximum SOC value, charging mode is activated. Considering the ECMS method, equivalent fuel consumption was calculated so that the SOC was the same at the beginning and end of the

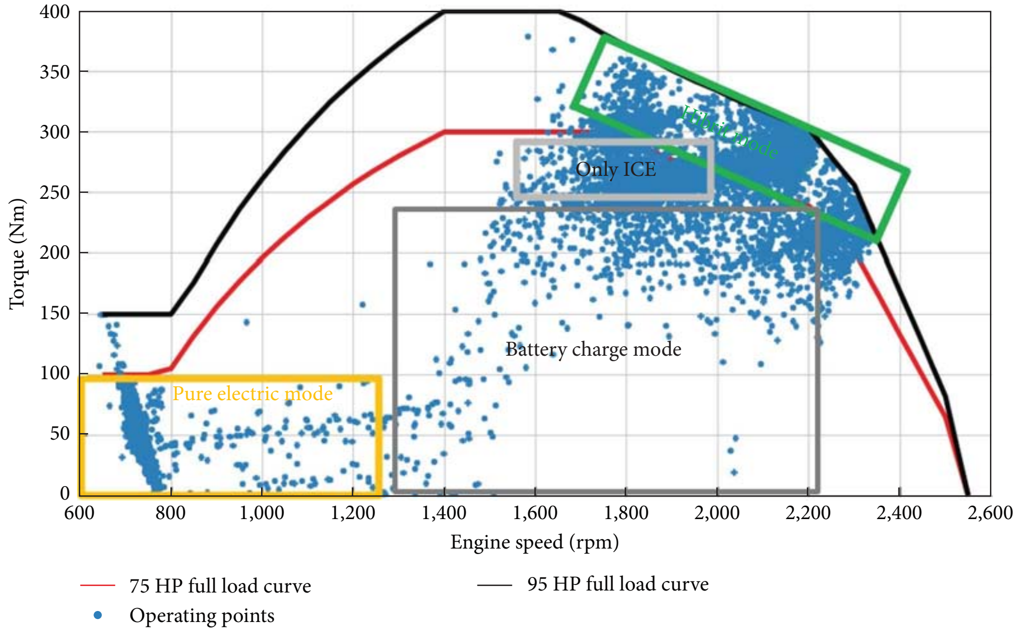

Figure 17: System operating region on engine map.

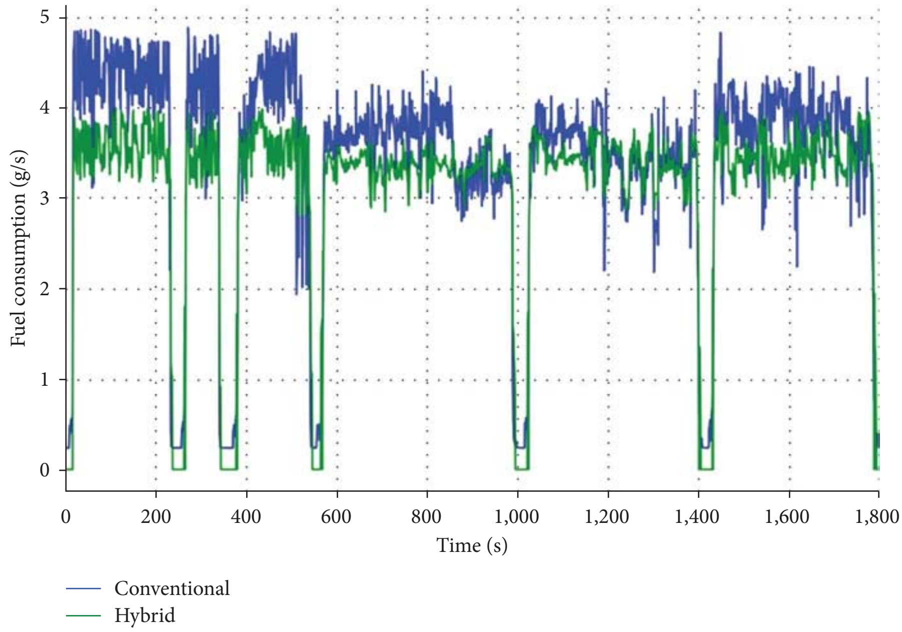

Figure 18: Fuel consumption of conventional and hybrid tractor.

cruise cycle. Under other partial load driving conditions the vehicle operates in hybrid mode. However, the full load curve of the 3-cylinder internal combustion engine in hybrid mode is affected by the engine's lower torque in the full load torque curve. Therefore, the full load curve is achieved by operating in hybrid mode with the assistance of the electric motor.

3. Results and Discussion

This section summarizes the simulation results for fuel consumption and emissions of an optimization-based energy management strategy tested on agricultural vehicles for ploughing operation.

3.1. Fuel Consumption. The fuel consumption of a tractor depends on several factors, including its size, load, and operating terrain [26]. The proposed strategy's fuel consumption is tested using real driving cycle data given in previously.

Figure 18 presents the comparison of the instantaneous fuel consumption rates between conventional and hybrid tractors. The results show that the hybrid drive system reduces the maximum fuel consumption from 4.88 to 4 g/s.

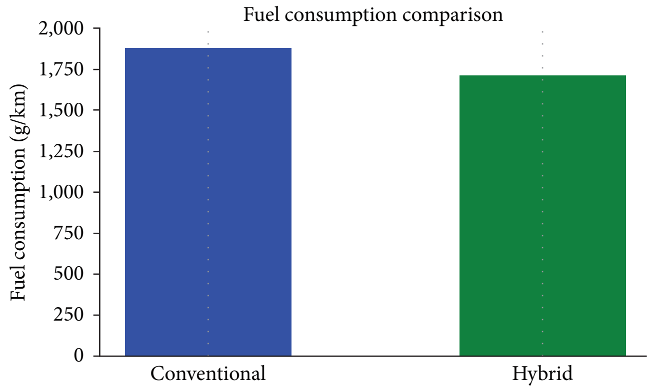

FIGURE 19: Total fuel consumption of conventional and hybrid tractors.

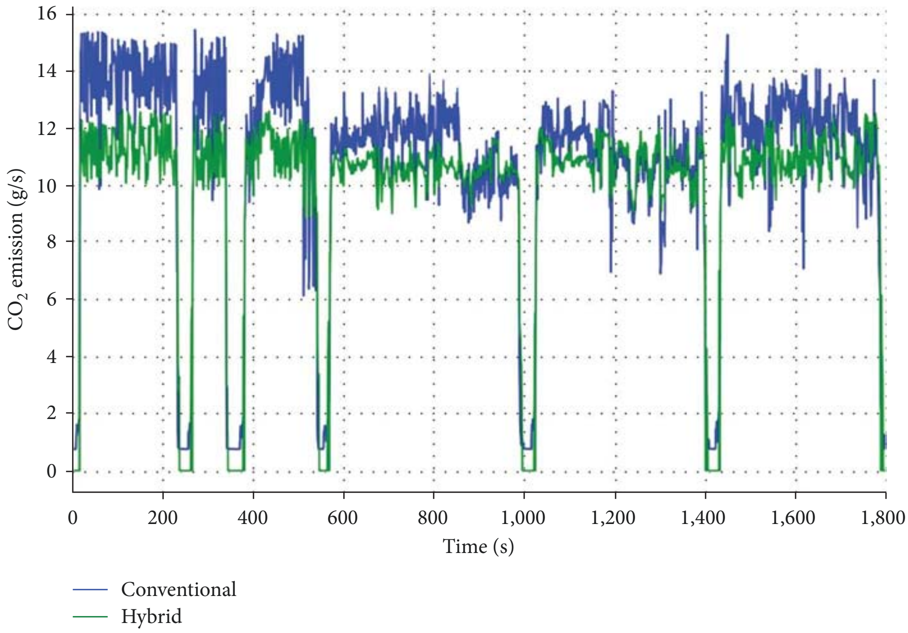

FIGURE 20: CO_2 emission of conventional and hybrid tractor.

The graph shows a significant improvement in instantaneous fuel consumption with the hybrid vehicle propulsion system. It can be seen that at almost all points, there is a significant improvement in the hybrid operating mode compared to the conventional operating mode. Significant decreases were observed in instantaneous fuel consumption values. A comparison of the instantaneous fuel consumption of hybrid and conventional vehicles reveals that the fuel consumption of the hybrid vehicle drive system is lower at almost all points.

Figure 19 presents the total fuel consumption data for the simulated vehicles. It is evident that the hybrid model has a lower fuel consumption than the conventional model, with fuel consumption rates of 1,880.1 and 1,712.5 g/km for the two configurations, respectively. This can be explained by the downsized engine used in the hybrid configuration. In addition, with the hybrid operating mode, it has been effective to work with the electric motor both in transient power demands and in partial loads and in more efficient regions on the motor map. Thus, working in inefficient regions of the low-power internal combustion engine is prevented. Both the hybrid operating mode and the ability to use a lower power engine due to the hybrid structure were effective in this situation. Another result obtained from the graph is higher speeds result in higher fuel consumption when driving on soil with the same characteristics, which aligns with findings in the literature [27, 28]. It has been shown that fuel consumption can be reduced by an average of 8% by using a hybrid drive-in tractors.

3.2. CO_2 Emission. A significant amount of the engine emissions that contribute to environmental issues are produced by work machinery, including forestry and agricultural tractors [29]. Tractors, which play a very important role in agricultural practices, are used in many processes such as ploughing, soil cultivation, planting, and fertilizer spreading [26]. The implementation area in which the tractor is used

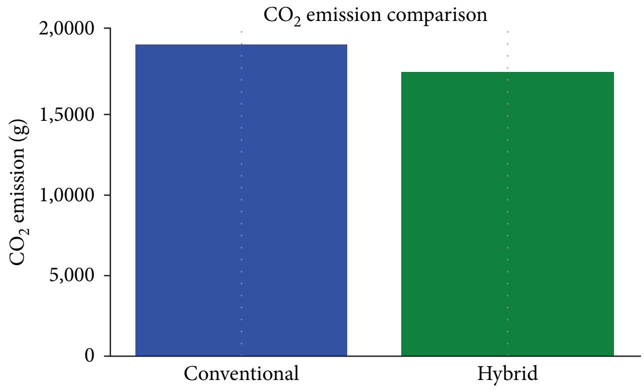

FIGURE 21: Total CO_2 emission of conventional and hybrid tractors.

and the choice of tractor type impacts engine emissions [30]. Engine speed and load also have an effect on emissions [31].

In the study, CO_2 emission rates of conventional and hybrid tractors in ploughing operations were measured and compared. Figure 20 demonstrates the instantaneous CO_2 emission rates of a vehicle with a conventional engine drive system and a hybrid vehicle with downsized engine for the drive cycle. When comparing a conventional tractor to a hybrid, the highest CO_2 emission is reduced from 15.45 to 12.64 g/s. This decrease corresponds to 18%. At almost all operating points, lower CO_2 emissions have been observed in hybrid mode. The main reasons for the decrease in hybrid operating mode are that the electric motor operates at more efficient points during transient power demands and the internal combustion engine operates at more efficient points.

Figure 21 shows total CO_2 emissions of conventional and hybrid vehicles. In the hybrid configuration, lower CO_2 emissions were observed compared to the conventional vehicle. The CO_2 emissions released into the environment were reduced by a total of 8.93%; 19,353 g for the conventional tractor and 17,623 g for the hybrid tractor. The main reason for the improvement in CO_2 emissions is that, with the hybrid operating strategy, transient power demands are met by the electric motor, and the downsized motor is operated in higher efficiency regions at partial loads.

The fuel consumption and CO_2 emission data indicate that it is feasible to downsize a tractor's internal combustion engine by integrating an electric motor into its architecture. Furthermore, electric motors enable greater flexibility in speed control, enabling more precise adherence to the target speed profile of the work cycle compared to a traditional tractor [32].

4. Conclusions

Using hybrid technology in tractors is a proven way of improving fuel economy and reducing environmental impact. Hybrid tractors maximize efficiency and reduce environmental impact without sacrificing performance by minimizing equivalent consumption. This aligns with the goal of sustainable farming practices, which prioritize minimizing resource consumption.

In the study, a model was developed and applied to estimate the fuel consumption and CO_2 emissions of conventional and hybrid tractors in ploughing operations. The transition from four to three cylinders is commercially beneficial as it improves weight, cost, and specific fuel consumption. The study concluded that the hybrid drive system operating under the ECMS method can achieve an 8.0% improvement in fuel consumption and a 8.9% reduction in CO_2 emissions compared to a conventional tractor.

More work is required to create novel, affordable, and energy-efficient technology and energy management strategies in order to encourage the commercial use of hybrid tractors.

Data Availability

The data that support the findings of this study are available from the corresponding author upon reasonable request.

Conflicts of Interest

The authors declare that they have no conflicts of interest.

Acknowledgments

The authors appreciate the support provided by TUMOSAN.

References

[1] S. Gorjian, O. Fakhraei, A. Gorjian, A. Sharafkhani, and A. Aziznejad, "Sustainable food and agriculture: employment of renewable energy technologies," *Current Robotics Reports*, vol. 3, no. 3, pp. 153–163, 2022.

[2] E. Scolaro, M. Beligoj, M. P. Estevez, L. Alberti, M. Renzi, and M. Mattetti, "Electrification of agricultural machinery: a review," *IEEE Access*, vol. 9, pp. 164520–164541, 2021.

[3] M. Gonzalez-de-Soto, L. Emmi, C. Benavides, I. Garcia, and P. Gonzalez-de-Santos, "Reducing air pollution with hybrid-powered robotic tractors for precision agriculture," *Biosystems Engineering*, vol. 143, pp. 79–94, 2016.

[4] H. Dou, H. Wei, Q. Ai, and Y. Zhang, "Optimal energy management strategy for dual-power coupling tractor based on the adaptive control technology," *PLoS ONE*, vol. 18, no. 11, Article ID e0292510, 2023.

[5] J. Li, X. Wu, X. Zhang, Z. Song, and W. Li, "Design of distributed hybrid electric tractor based on axiomatic design and extenics," *Advanced Engineering Informatics*, vol. 54, Article ID 101765, 2022.

[6] F. Mocera and V. Martini, "Numerical performance investigation of a hybrid eCVT specialized agricultural tractor," *Applied Sciences*, vol. 12, no. 5, Article ID 2438, 2022.

[7] M. A. Baba, M. Labbadi, M. Cherkaoui, and M. Maaroufi, "Fuel cell electric vehicles: a review of current power electronic converters Topologies and technical challenges," *IOP Conference Series: Earth and Environmental Science*, vol. 785, no. 1, Article ID 012011, 2021.

[8] J. J. Jui, M. A. Ahmad, M. M. I. Molla, and M. I. M. Rashid, "Optimal energy management strategies for hybrid electric vehicles: a recent survey of machine learning approaches," *Journal of Engineering Research*, 2024.

[9] Y. Cao, M. Yao, and X. Sun, "An overview of modelling and energy management strategies for hybrid electric vehicles," *Applied Sciences*, vol. 13, no. 10, Article ID 5947, 2023.

[10] M. Liu, Y. Li, L. Xu, Y. Wang, and J. Zhao, "General modeling and energy management optimization for the fuel cell electric

tractor with mechanical shunt type," *Computers and Electronics in Agriculture*, vol. 213, Article ID 108178, 2023.
[11] R. Guo, X. Xue, Z. Sun, and Z. Hong, "Clustered energy management strategy of plug-in hybrid electric logistics vehicle based on gaussian mixture model and stochastic dynamic programming," *IEEE Transactions on Transportation Electrification*, vol. 9, no. 2, pp. 3177–3191, 2023.
[12] F. Yue, Q. Liu, Y. Kong, J. Zhang, and N. Xu, "A predictive energy management strategy for multi-energy source vehicles based on full-factor trip information," *Sensors*, vol. 22, no. 1, Article ID 23, 2022.
[13] Y. Liu, J. Liu, Y. Zhang, Y. Wu, Z. Chen, and M. Ye, "Rule learning based energy management strategy of fuel cell hybrid vehicles considering multi-objective optimization," *Energy*, vol. 207, Article ID 118212, 2020.
[14] C. Yang, M. Zha, W. Wang, K. Liu, and C. Xiang, "Efficient energy management strategy for hybrid electric vehicles/plug-in hybrid electric vehicles: review and recent advances under intelligent transportation system," *IET Intelligent Transport Systems*, vol. 14, no. 7, pp. 702–711, 2020.
[15] Z. Zhu, L. Zeng, L. Chen, R. Zou, and Y. Cai, "Fuzzy adaptive energy management strategy for a hybrid agricultural tractor equipped with HMCVT," *Agriculture*, vol. 12, no. 12, Article ID 1986, 2022.
[16] L. J. Zhu, "Experiment for a parallel hydraulic hybrid terminal tractor," *Applied Mechanics and Materials*, vol. 543–547, pp. 211–214, 2014.
[17] S. Xie, X. Hu, S. Qi, and K. Lang, "An artificial neural network-enhanced energy management strategy for plug-in hybrid electric vehicles," *Energy*, vol. 163, pp. 837–848, 2018.
[18] C. Jia, W. Qiao, and L. Qu, "Numerical methods for optimal control of hybrid electric agricultural tractors," in *2019 IEEE Transportation Electrification Conference and Expo (ITEC)*, pp. 1–6, IEEE, Detroit, MI, USA, 2019, June.
[19] J. Han, A. Khalatbarisoltani, Y. Yang, and X. Hu, "Energy management in plug-in hybrid electric vehicles: preheating the battery packs in low-temperature driving scenarios," *IEEE Transactions on Intelligent Transportation Systems*, vol. 25, no. 2, pp. 1978–1991, 2024.
[20] J. Han, W. Liu, Y. Zheng, A. Khalatbarisoltani, Y. Yang, and X. Hu, "Health-conscious predictive energy management strategy with hybrid speed predictor for plug-in hybrid electric vehicles: Investigating the impact of battery electro-thermal-aging models," *Applied Energy*, vol. 352, Article ID 121986, 2023.
[21] H.-S. Lee, J.-S. Kim, Y.-I. Park, and S.-W. Cha, "Rule-based power distribution in the power train of a parallel hybrid tractor for fuel savings," *International Journal of Precision Engineering and Manufacturing-Green Technology*, vol. 3, no. 3, pp. 231–237, 2016.
[22] H. Dou, H. Wei, Y. Zhang, and Q. Ai, "Configuration design and optimal energy management for coupled-split powertrain tractor," *Machines*, vol. 10, no. 12, Article ID 1175, 2022.
[23] Q. Zhang and S. Tian, "Energy consumption prediction and control algorithm for hybrid electric vehicles based on an equivalent minimum fuel consumption model," *Sustainability*, vol. 15, no. 12, Article ID 9394, 2023.
[24] A. K. Gautam, M. Tariq, J. P. Pandey, K. S. Verma, and S. Urooj, "Hybrid sources powered electric vehicle configuration and integrated optimal power management strategy," *IEEE Access*, vol. 10, pp. 121684–121711, 2022.
[25] Y. Yang, Y. Zhang, J. Tian, and T. Li, "Adaptive real-time optimal energy management strategy for extender range electric vehicle," *Energy*, vol. 197, Article ID 117237, 2020.
[26] V. Van linden and L. Herman, "A fuel consumption model for off-road use of mobile machinery in agriculture," *Energy*, vol. 77, pp. 880–889, 2014.
[27] C. M. Kichler, J. P. Fulton, R. L. Raper, T. P. McDonald, and W. C. Zech, "Effects of transmission gear selection on tractor performance and fuel costs during deep tillage operations," *Soil and Tillage Research*, vol. 113, no. 2, pp. 105–111, 2011.
[28] N.-L. Vu, P. Messier, B. H. Nguy n et al., "Energy-optimization design and management strategy for hybrid electric non-road mobile machinery: a case study of snowblower," *Energy*, vol. 284, Article ID 129249, 2023.
[29] P.-A. Hansson, M. Lindgren, and O. Norén, "A comparison between different methods of calculating average engine emissions for agricultural tractors," *Journal of Agricultural Engineering Research*, vol. 80, no. 1, pp. 37–43, 2001.
[30] G. Rashid, R. Hekmat, L. A. Nejat, and J. Payam, "Analysis and comparison exhaust gas emissions from agricultural tractors," *International Journal of Agriculture and Crop Sciences*, vol. 5–7, pp. 688–694, 2013.
[31] S. K. Pitla, J. D. Luck, J. Werner, N. Lin, and S. A. Shearer, "In-field fuel use and load states of agricultural field machinery," *Computers and Electronics in Agriculture*, vol. 121, pp. 290–300, 2016.
[32] S. Pascuzzi, K. Lyp-Wronska, K. Gdowska, and F. Paciolla, "Sustainability evaluation of hybrid agriculture-tractor powertrains," *Sustainability*, vol. 16, no. 3, Article ID 1184, 2024.